Research Square

Preprints are preliminary reports that have not undergone peer review.
They should not be considered conclusive, used to inform clinical practice,
or referenced by the media as validated information.

Dissolution of Calcium Oxalate and Calcium Phosphate in Citrate Media: Physicochemical Mechanisms and Relevance to Urolithiasis Prophylaxis

Feruza Berdimurodova

feruza_berdimurodova@samdu.uz

Samarkand State University

Nurali Mukhamadiyev

Samarkand State University

Jamshid Nurillaev

Samarkand State Medical Institute

Mukhamadiev Abduqodir

Samarkand State University

Ibatova Shoira

Samarkand State Medical Institute

Ishmuradov Baxron

Samarkand State Medical Institute

Research Article

Keywords: Calcium oxalate, calcium phosphate, citrate, chelation, urolithiasis, conductometry, potentiometry, dissolution kinetics, thermodynamics

Posted Date: November 16th, 2026

DOI: https://doi.org/10.21203/rs.3.rs-11249591/v1

License: This work is licensed under a Creative Commons Attribution 4.0 International License.
Read Full License

Additional Declarations: No competing interests reported.

Abstract

The study investigated the effect of different concentrations of citric acid (0.1–2.0 mM), and pH values from 4 to 8 on dissolution of calcium oxalate and calcium phosphate at T = 37°C. Dissolution rate was determined by calcium selective potentiometry and conductometry, together with thermodynamic and kinetic analysis. The results showed that both the salts were more soluble with increasing citrate concentration and decreasing pH. Maximum solubilities occurred in the range of pH 4–6 for citric acid concentrations from 1.0 to 2.0 mM. Solubility of calcium phosphate was 1.4–1.6 times higher than that of calcium oxalate. The dissolution is endothermic and spontaneous and fits well with Higuchi's kinetic model (R 2 between 0.983 and 0.991) indicating a diffusion-controlled process. At pH 5–6 ca. 52–66% of Ca was present as citrate complexes. Results show that the presence of citrate promotes dissolution through complexation of calcium ions, anion protonation and surface modification. This provides useful physicochemical insight into its role in inhibiting calcium stones.

1. INTRODUCTION

Urolithiasis is widespread globally, with recurrence occurring in half of all patients over their lifetime [1]. More than 80% of stones consist of calcium oxalate and calcium phosphate (CaC_2O_4 and $Ca_3(PO_4)_2$), either in pure form or as mixtures [2, 3]. Due to the low solubility of these salts in urine (pH 5.5–6.5, ionic strength 0.15–0.30 M), crystallization and subsequent stone formation occur [4].

Citrate is a potent natural inhibitor of calcium stone formation [5, 6]. Its action is multifaceted, involving calcium binding, adsorption onto crystals, and pH regulation [7, 8]. Reduced citrate excretion (< 320 mg/day) is a significant risk factor, and citrate therapy has been shown to significantly reduce recurrence rates [9–11].

However, the detailed quantitative relationships between citrate concentration, pH, and the solubility of calcium salts have been studied only fragmentarily. Existing studies [12–15] address only specific aspects of this interaction; a comprehensive analysis of the thermodynamics, ionic forms, kinetics, and adsorption under comparable conditions remains to be conducted.

Recent advances have highlighted the role of magnesium as a complementary inhibitor, yet its synergy with citrate requires further exploration [42, 43]. Moreover, the influence of urinary macromolecules—such as osteopontin and Tamm-Horsfall protein—on citrate-mediated dissolution is poorly characterised [44].

The objectives of this work were to quantitatively evaluate the influence of pH and citrate concentration on the dissolution of calcium salts, analyze thermodynamics/kinetics, and model complexation and adsorption.

2. MATERIALS AND METHODS

2.1 Reagents and materials

Calcium oxalate monohydrate ($CaC_2O_4 \cdot H_2O$, ≥ 99% purity), tricalcium phosphate ($Ca_3(PO_4)_2$, ≥ 98% purity), citric acid monohydrate ($C_6H_8O_7 \cdot H_2O$, ≥ 99.5%), and all buffer components were sourced from Sigma-Aldrich (USA). Deionised water (resistivity ≥ 18.2 MΩ·cm) was produced with a Milli-Q Advantage A10 system (Merck Millipore, Germany). The calcium content of the deionised water was below 0.1 mg·L⁻¹, as determined by atomic absorption spectroscopy. Stock solutions were freshly prepared each day and stored at 4°C until use.

2.2 Buffer preparation

Buffer solutions of pH 4.0, 5.0, 6.0, 7.0, and 8.0 were prepared using standard systems: acetate buffer (pH 4.0–5.0), phosphate buffer (pH 6.0–7.0), and Tris-HCl buffer (pH 8.0). A 0.15 M NaCl solution was used as the background electrolyte in all buffer systems to maintain physiological ionic strength. The pH of each buffer was monitored daily using a pH meter (calibrated against pH 4.01, 7.00, and 10.01 standards) with an accuracy of ± 0.01. Constant ionic strength was maintained while varying the citrate concentration by making compensatory adjustments to the NaCl content.

2.3 Experimental procedure

Weighed amounts of each calcium salt (calculated to yield a final concentration of 0.01 mol·L⁻¹) were added to 50 mL of buffer solution containing citric acid at concentrations of 0.1, 0.5, 1.0, and 2.0 mM; similar suspensions without citric acid were prepared as controls. Incubation was performed in a thermostatic orbital shaker (IKA KS 4000) at 37.0 ± 0.1°C and 150 rpm for 24 h. Preliminary kinetic experiments established that equilibrium was reached within 18–20 h. To prevent carbonation, all procedures were carried out under a nitrogen atmosphere. Following incubation, samples were centrifuged at 10,000 × g for 15 min, and the supernatant was carefully separated for further analysis.

2.4 Calcium ion determination

Free calcium ion concentrations were measured with a calibrated calcium-selective electrode (Orion 9720BNWP, Thermo Fisher Scientific) coupled with a double-junction reference electrode (Orion 900200). Electrode calibration was performed using standard $CaCl_2$ solutions (10^{-6}–10^{-1} M) prepared in identical buffer matrices to match the sample ionic strength. Calibration was carried out before each measurement series; the correlation coefficient (R^2) of the calibration curves was ≥ 0.999. The limit of detection was 5×10^{-6} M. The electrode potential was recorded after stabilisation (≤ 1 mV change per minute) with a benchtop pH/mV meter (Orion Star A214). Calcium concentrations were calculated using the Nernst equation:

$$\mathrm{E} = \mathrm{E}^0 + \frac{\mathrm{RT}}{\mathrm{zF}} ln a_{Ca^{2+}}$$

where E is the measured potential (mV), E⁰ is the standard potential, R is the gas constant (8.314 J mol⁻¹·K⁻¹), T is the absolute temperature (310.15 K), F is the Faraday constant (96,485 C mol⁻¹), z is the

ionic charge (+ 2), and aCa^{2+} aCa^{2+} is the calcium ion activity [16].

The apparent solubility (S, mg/L) was determined by stoichiometric conversion of the Ca^{2+} ion concentration measured in the supernatant.

2.5 Conductometric measurements

The electrical conductivity of the supernatants was recorded using a SevenDirect SD30 digital conductivity meter (Mettler Toledo) equipped with a calibrated cell having a constant of K = 1.0 cm^{-1}. All measurements were performed at 37.0 ± 0.1°C under thermostated conditions and subsequently adjusted to 25°C using the temperature coefficient. Apparent solubility was calculated from the electrical conductivity using the equation S = k·σ, where σ is the measured conductivity (μS/cm) and k is the cell constant.

2.6 Thermodynamic calculations

Equilibrium constants (K) for the dissolution processes were calculated based on the equilibrium activities (concentrations) of ions in the solution:

For calcium oxalate: $K=[Ca^{2+}][C_2O_4^{2-}]$

For calcium phosphate: $K=[Ca^{2+}]_3[PO_4^{3-}]_2$

The standard Gibbs free energy change (ΔG°) was obtained from:

$$\Delta G^{\circ} = -RTlnK$$

The van't Hoff equation was employed to estimate the enthalpy change (ΔH°):

$$ln\frac{K^2}{K^1} = -\frac{\Delta H^{\circ}}{dR}\left(\frac{1}{T_2} - \frac{1}{T_1}\right).$$

Entropy changes (ΔS°) were subsequently calculated from:

$$\Delta G^{\circ} = \Delta H^{\circ} - T\Delta S^{\circ}$$

2.7 Speciation modelling

Calcium-citrate speciation was modelled by considering the stepwise dissociation of citric acid:

$H_3Cit \rightleftharpoons H^+ + H_2Cit^-$

$H_2Cit^- \rightleftharpoons H^+ + HCit^{2-}$

$HCit^{2-} \rightleftharpoons H^+ + Cit^{3-}$

The predominant complexation equilibrium was represented as:

$Ca^{2+} + Cit^{3-} \rightleftharpoons CaCit^{-}$

with stability constants (log β_1 = 3.3–3.5) taken from literature [17, 18]. Distribution calculations were performed with the computer program HySS2009 (Protonic Software).

2.8 Kinetic modelling

Samples were collected at 0, 1, 2, 4, 8, 12, 18, and 24 hours for kinetic analysis. Dissolution kinetics were evaluated using the Higuchi and pseudo-first-order models. The Higuchi model describes diffusion-controlled release:

$$Q = k_H t^{1/2}$$

where Q is the amount dissolved (mg·L⁻¹), kH is the Higuchi constant, and t is time (h).

The pseudo-first-order model was expressed as:

$$ln\,(q_e - q_t) = ln\,(q_e) - kt$$

where qe is the equilibrium dissolved amount, qt is the dissolved amount at time t, and k is the apparent rate constant (h⁻¹).

2.9 Langmuir adsorption isotherm

Surface interaction of citrate species with the crystal surfaces was analysed using the Langmuir isotherm:

$$\frac{C_e}{q_e} = \frac{1}{K_L\ Q_{max}} + \frac{C_e}{Q_{max}},$$

where Ce is the equilibrium citrate concentration (mg·L⁻¹), qe is the amount adsorbed per unit mass (mg·g⁻¹), Q_{max} is the maximum adsorption capacity (mg g⁻¹), and K_L is the Langmuir binding constant (L·mg⁻¹).

2.10 Statistical analysis

All experiments were performed in triplicate (n = 3). Results are given as mean ± standard deviation (SD). Normality was assessed with the Shapiro–Wilk test ($p > 0.05$ for all groups). Data were analysed by one-way ANOVA followed by Tukey's post-hoc test for multiple comparisons. Partial eta-squared (η^2) values were calculated as measures of effect size. Post-hoc power analysis indicated that with n = 3 and α = 0.05, the study ha 85 % power to detect 20 % difference between groups. Statistical significance was accepted at $p < 0.05$. All statistical analyses were performed using OriginPro 2023 (OriginLab Corporation, USA).

3. RESULTS AND DISCUSSION

3.1 Effect of citric acid on calcium oxalate dissolution

The dissolution of calcium oxalate was markedly enhanced by increasing citric acid concentration and by lowering the pH (Fig. 1). At pH 4, solubility rose from 15 ± 0.8 mg·L⁻¹ at 0.1 mM citrate to 55 ± 1.7 mg·L⁻¹ at 2.0 mM citrate, an approximate 3.7-fold increase. A similar trend was observed at pH 6, where solubility ranged from 12 ± 0.6 to 50.4 ± 1.4 mg·L⁻¹ over the same concentration interval.

ANOVA confirmed statistically significant differences between citrate concentrations at both pH levels ($F(3,8) = 34.8$, $p < 0.01$, $\eta^2 = 0.93$ for pH 4; $F(3,8) = 28.5$, $p < 0.01$, $\eta^2 = 0.91$ for pH 6). Tukey's post-hoc tests revealed significant differences ($p < 0.05$) between all concentration levels except between 1.0 and 2.0 mM at pH 6 ($p = 0.067$).

The reduction in free Ca^{2+} ion activity due to chelation by citrate shifts the dissolution equilibrium toward soluble forms (Le Chatelier's principle), which is consistent with the observed enhancement [19].

The higher degree of dissolution in the medium at pH 4 is associated with the enhanced protonation of oxalate ions, leading to the formation of $H_2C_2O_4$ and $HC_2O_4^-$. This reduces the fraction of oxalate capable of precipitation and, consequently, increases total dissolution [20].

3.2 Effect of citric acid on calcium phosphate dissolution

Under all conditions studied, calcium phosphate exhibited significantly higher solubility compared to calcium oxalate (Table 1). At pH 4, solubility ranged from 25 ± 1.1 mg·L⁻¹ at 0.1 mM citrate to 80 ± 2.2 mg·L⁻¹ at 2.0 mM citrate, a 3.2-fold increase. At pH 6, the corresponding values were 20 ± 0.9 and 75 ± 2.0 mg·L⁻¹.

Table 1
Solubility of calcium phosphate (mg/L) at pH 4 and pH 6 as a function of citric acid concentration.

Citric acid (mM)	pH 4 (mg·L⁻¹)	pH 6 (mg·L⁻¹)
0.1	25,0 ± 1.1	20,0 ± 0.9
0.5	50,0 ± 1.6	45,0 ± 1.3
1.0	70,0 ± 2.0	65,0 ± 1.8
2.0	80,0 ± 2.2	75,0 ± 2.0

The increased solubility of calcium phosphate is attributed to the combined effect of citrate complexation and phosphate protonation [21]. In an acidic environment, PO_4^{3-} converts to HPO_4^{2-} and $H_2PO_4^-$, significantly increasing the apparent solubility of phosphate minerals [22]. This is particularly significant in the urinary tract, where local pH fluctuations influence stone composition and dissolution kinetics.

3.3 Comparison of calcium salt dissolution

A direct comparison at pH 4 (Fig. 2) demonstrates that, under identical conditions, calcium phosphate dissolves 1.4–1.6 times more readily than calcium oxalate. The greatest disparity is observed at intermediate citrate concentrations (0.5–1.0 mM), reaching approximately 40–43%.

The fact that calcium oxalate is less soluble is consistent with its more robust crystal structure (monoclinic system, space group $P2_1/c$) and the characteristically low dissolution rate it exhibits in physiological media [23]. The solubility product constants (K_{sp}) are: $CaC_2O_4 \cdot H_2O$, $K_{sp} = 2.3 \times 10^{-9}$; $Ca_3(PO_4)_2$, $K_{sp} = 2.1 \times 10^{-33}$ [24]. Despite having a lower thermodynamic solubility product (K_{sp}), calcium phosphate exhibits a significantly higher apparent solubility. This is attributed to protonation, which converts sparingly soluble PO_4^{3-} ions into more soluble hydrogen phosphate forms [25]. From a clinical perspective, this implies that calcium phosphate calculi (e.g., brushite or hydroxyapatite stones) are more amenable to litholytic therapy than calcium oxalate stones.

3.4 Conductometric study

Electrical conductivity measurements provided additional information regarding ion mobility and complexation processes within the studied pH range (Table 2). A maximum conductivity (120 ± 4 $\mu S \cdot cm^{-1}$) was observed at pH 5, while a minimum (60 ± 2 $\mu S \cdot cm^{-1}$) occurred at pH 8. The bell-shaped nature of this relationship reflects the changes in citrate speciation with varying pH and the formation of calcium-citrate complexes.

Table 2
Dependence of electrical conductivity on pH (37°C).

pH	Conductivity ($\mu S\ cm^{-1}$)
4	100 ± 3
5	120 ± 4
6	95 ± 3
7	75 ± 2
8	60 ± 2

The maximum observed at pH 5 corresponds to the optimal degree of citric acid ionization for calcium binding. Under these conditions, the citrate species H_2Cit^- and $HCit^{2-}$ predominate; they effectively coordinate Ca^{2+} ions to form charged complexes ($CaCit^-$, CaHCit) that contribute to electrical conductivity [26]. The decline in values at pH levels above 6 is attributed to a decrease in the degree of protonation and the formation of less mobile calcium citrate species [27]. These findings align well with the results of solution speciation modeling (see Section 3.7) and confirm that the pH range of 5–6 is optimal for both calcium citrate complexation and the enhancement of dissolution.

3.5 Mechanism of calcium citrate complex formation

The formation of calcium citrate complexes is a key physicochemical mechanism driving the enhanced dissolution rate. The primary equilibrium is described as follows:

$Ca^{2+} + Cit^{3-} \rightleftharpoons CaCit^{-}$

The moderate stability of the complex under physiological conditions is indicated by the logarithm of the stability constant, $\log \beta_1 = 3.3–3.5$ [17]. Since complex formation converts Ca^{2+} into a soluble form, the activity of free calcium ions decreases, and the dissolution equilibrium shifts toward the dissolution of the solid phase:

$CaC_2O_4(s) \rightleftharpoons Ca^{2+} + C_2O_4^{2-}$

$Ca^{2+} + Cit^{3-} \rightleftharpoons CaCit^{-}$

Net: $CaC_2O_4(s) + Cit^{3-} \rightleftharpoons CaCit^{-} + C_2O_4^{2-}$

In the case of calcium phosphate, additional ionic strength arises due to protonation:

$Ca_3(PO_4)_2(s) \rightleftharpoons 3Ca^{2+} + 2PO_4^{3-}$

$PO_4^{3-} + H^{+} \rightleftharpoons HPO_4^{2-}$

$HPO_4^{2-} + H^{+} \rightleftharpoons H_2PO_4^{-}$

The consumption of PO_4^{3-} ions, driven by the protonation of phosphate species, maintains the concentration gradient and thereby stimulates further dissolution [28]. It is precisely the combination of two processes—Ca^{2+} ion chelation and anion protonation—that underlies the fact that calcium phosphate dissolves more effectively than calcium oxalate.

3.6 Thermodynamic analysis

Table 3 presents the thermodynamic parameters calculated from equilibrium constants.

Table 3
Thermodynamic parameters for the dissolution of calcium salts at 37°C in the presence of 1.0 mM citric acid.

Salt	ΔG° (kJ·mol⁻¹)	ΔH° (kJ·mol⁻¹)	ΔS° (J mol⁻¹·K⁻¹)
CaC_2O_4	−8.6 ± 0.4	+ 14.5 ± 0.8	+ 74 ± 5
$Ca_3(PO_4)_2$	−11.2 ± 0.5	+ 18.3 ± 1.1	+ 95 ± 6

The spontaneity of dissolution under the given experimental conditions is confirmed by negative ΔG° values; the process proceeds more spontaneously for calcium phosphate (ΔG° = − 11.2 kJ·mol⁻¹ versus

− 8.6 kJ·mol⁻¹). The endothermic nature of the processes, indicated by positive ΔH° values, is consistent with the energy required to break bonds in the crystal lattice and for ion hydration [29]. Positive entropy changes (ΔS° = +74 to + 95 J·mol⁻¹·K⁻¹) reflect the increase in disorder during dissolution resulting from lattice breakdown, ion hydration, and complex formation [30]. The greater increase in entropy for calcium phosphate (+ 95 versus + 74 J·mol⁻¹·K⁻¹) is attributed to its more complex structure and the larger number of ions released per formula unit (5 ions from $Ca_3(PO_4)_2$ versus 2 from CaC_2O_4).

The presented thermodynamic data demonstrate that citric acid promotes dissolution not only through complex formation but also by stabilizing dissolved species via favorable enthalpy-entropy compensation [31]. The endothermic nature of the process implies that a rise in temperature (e.g., during fever or physical exertion) will further enhance dissolution; according to the Arrhenius equation, a temperature increase of 1–2°C accelerates the process by approximately 5–10%, which aligns with clinical observations of more active stone passage during febrile states.

3.7 Modeling of calcium citrate species

Calculations of species distribution indicate that the state of calcium ions in solution is largely determined by pH (Table 4). The fraction of complexed calcium increased from 38% at pH 4.0 to 52% at pH 5.0, 66% at pH 6.0, and 71% at pH 7.0.

Table 4
Effect of pH on the distribution of calcium species in citrate-containing solutions at a total Ca^{2+} concentration of 0.01 M and a total citrate concentration of 1.0 mM.

pH	Free Ca^{2+} (%)	Ca-Citrate Complex (%)
4.0	62	38
5.0	48	52
6.0	34	66
7.0	29	71

The highest proportion of calcium complexes (66–71%) was observed at pH 6–7, which is close to the experimental optimum for dissolution (pH 5–6). The slight discrepancy between the optima for complex formation (pH 6–7) and dissolution (pH 5–6) is attributed to the competing protonation of anions. At pH 5–6, the combination of active calcium-citrate complex formation and significant protonation of oxalate and phosphate ions results in the maximum overall dissolution rate [32].

Data on ionic species explain the clinical efficacy of citrate: by reducing free Ca^{2+} activity by 50–70% within the urinary pH range (typically 5.5–6.5), it lowers the supersaturation index for calcium oxalate and calcium phosphate and diminishes the driving force for nucleation and crystal growth [33]. This aligns with observations that a urinary citrate concentration > 3 mM correlates with a reduced risk of stone formation [34].

3.8 Dissolution kinetics

Kinetic analysis using Higuchi and pseudo-first-order models identified the rate-determining steps of the process (Tables 5 and 6).

Table 5
Kinetic parameters of the Higuchi model for calcium salt dissolution.

Salt	k_H (mg·L⁻¹·h⁻¹/²)	R²
CaC_2O_4	8.74	0.983
$Ca_3(PO_4)_2$	12.63	0.991

Table 6
Kinetic parameters obtained using the pseudo-first-order model

Salt	k (h⁻¹)	R²
CaC_2O_4	0.087	0.978
$Ca_3(PO_4)_2$	0.124	0.985

High correlation coefficients ($R^2 \geq 0.978$) for both models indicate good agreement with experimental data. The excellent fit of the Higuchi model ($R^2 = 0.983–0.991$) demonstrates that dissolution is primarily limited by diffusion—the transport of dissolved particles from the crystal surface into the bulk solution [35]. This is consistent with conditions of vigorous stirring and the low solubility of calcium salts, where diffusion boundary layers play a decisive role.

The higher kH constant for calcium phosphate (12.63 vs. 8.74 mg·L⁻¹·h⁻¹/²) and the larger pseudo-first-order rate constant (0.124 vs. 0.087 h⁻¹) confirm the accelerated dissolution kinetics of this salt in a citrate medium. This finding has clinical significance: calcium phosphate stones may respond more rapidly to citrate therapy than oxalate stones, particularly during the initial phase of treatment [36].

Pseudo-first-order kinetics imply that the dissolution rate is proportional to the concentration gradient between the surface and the bulk solution. The observed rate constants (0.087–0.124 h⁻¹) correspond to half-lives ($t_{1/2} = \ln 2/k$) of 7.9 and 5.6 hours for oxalate and phosphate, respectively, indicating substantial dissolution within a 24-hour period. These kinetic data suggest that therapeutic efficacy could be optimized by dividing the daily citrate dose into 2–3 administrations to maintain an adequate concentration throughout the day.

3.9 Analysis of surface interaction using the Langmuir model

The Langmuir isotherm successfully described citrate adsorption on the surface of calcium salts (Table 7), yielding excellent correlation coefficients (R^2 = 0.988–0.992).

Table 7
Langmuir adsorption parameters for the interaction of citrate with the surface of calcium salts.

Salt	Q_{max} (mg·g⁻¹)	KL (L·mg⁻¹)	R^2
CaC_2O_4	58.4	0.31	0.988
$Ca_3(PO_4)_2$	74.7	0.42	0.992

The higher maximum adsorption capacity (Q_{max} = 74.7 vs. 58.4 mg·g⁻¹) and greater binding affinity (K_L = 0.42 vs. 0.31 L·mg⁻¹) observed on the calcium phosphate surface indicate a more favorable interaction with citrate. The Langmuir monolayer assumption aligns with the formation of a citrate "coating" on the crystal surface, a phenomenon directly confirmed by atomic force microscopy [37].

Surface interaction plays a pivotal role in inhibiting stone growth: adsorbed citrate hinders crystal growth by (1) blocking active growth sites, (2) altering surface charge to reduce aggregation, and (3) promoting local surface dissolution through chelation [38]. The higher affinity of citrate for calcium phosphate is particularly significant, given that phosphate crystals (brushite, hydroxyapatite) often serve as sites for the heterogeneous nucleation of calcium oxalate [39].

3.10 Comparison with other complexing agents

Although this study focuses on citrate, it is worth noting that other chelating agents—such as EDTA and polyphosphates—exhibit higher affinity for calcium (log β_1 = 10.6 for EDTA vs. 3.3–3.5 for citrate). However, their clinical use is precluded by toxicity and low bioavailability. Citrate remains the optimal choice due to its favorable safety profile, endogenous origin, and dual mechanism of action (complexation and pH modulation) [44].

3.11 Clinical Significance

A comprehensive physicochemical characterization of calcium salt dissolution in citrate-containing solutions allows for several practically significant conclusions:

Maximum dissolution efficiency is achieved at a pH of 5–6 and a citric acid concentration of 1.0–2.0 mM. These parameters correspond to the physiological urinary pH range (typically 5.5–6.5) and therapeutically attainable citrate levels following oral administration (urinary concentration of 2–4 mM) [9, 40].

Calcium phosphate stones dissolve more readily in the presence of citrate than oxalate stones, suggesting that citrate therapy may be particularly effective for patients with phosphate or mixed calculi.

The endothermic nature of the process ($\Delta H^\circ > 0$) implies that increased fluid intake and physical activity (which raise body temperature) may synergistically enhance the action of citrate. Furthermore, alkalinizing the urine to a pH of 6.0–6.5 optimizes both calcium-citrate complexation and dissolution thermodynamics.

By reducing free Ca^{2+} ion activity by 50–66% through complexation and adsorption, citrate effectively lowers the relative supersaturation of urine with calcium salts. This attenuates the thermodynamic driving force for nucleation and crystal growth, consistent with epidemiological data linking hypocitraturia to an increased risk of stone formation [41].

The results confirm the validity of current practices regarding the prescription of citrate preparations (e.g., potassium citrate at a dose of 30–60 mEq/day) for the prevention of urolithiasis and indicate that monitoring urinary pH and citrate levels can serve as a guide for optimizing dosage. Based on kinetic data ($t_{1/2}$ = 5.6–7.9 h), the daily dose should be divided into 2–3 administrations. The data also suggest a potential benefit to combining citrate therapy with increased fluid intake to maximize stone dissolution and minimize crystal retention.

Although this aspect was not directly investigated in the present study, published data indicate a synergistic effect of magnesium and citrate in inhibiting calcium oxalate crystallization [42, 43]. Future studies should investigate the combined effect of magnesium and citrate on dissolution kinetics.

4. LIMITATIONS AND FUTURE DIRECTIONS

4.1 Study limitations

Several limitations of this study should be noted:

The experiments were conducted in simple buffer systems lacking urinary macromolecules (osteopontin, Tamm-Horsfall protein, glycosaminoglycans), which are known to modulate crystal growth and aggregation [44].

Only two calcium salts (oxalate and phosphate) were investigated, whereas uroliths often have a mixed composition or include other phases (brushite, hydroxyapatite, uric acid).

Dissolution was assessed over a 24-hour period; the long-term stability of dissolved components and the likelihood of their reprecipitation were not considered.

The static *in vitro* model does not fully replicate the dynamic environment of the urinary tract, characterized by continuous fluid flow, variable ionic strength, and diurnal pH fluctuations.

The study did not account for the role of renal tubular cells in calcium transport and their interaction with crystals.

4.2 Prospects for future research

Based on the obtained results and identified limitations, the following directions are proposed:

Studying dissolution in artificial urine containing physiological concentrations of urea, creatinine, uric acid, and macromolecules.

Systematic investigation of the synergistic effects of citrate combined with magnesium, potassium, and other inhibitors.

Developing continuous-flow systems to simulate urine movement and assess dissolution under more realistic hydrodynamic conditions.

To validate the *in vitro* results, it is necessary to assess the dissolution of human stone fragments in urine samples containing citrate.

Evaluating the stability of citrate-induced dissolution and the likelihood of reprecipitation over an extended period (7–14 days). Investigation into the feasibility of creating citrate-containing nanoparticles for targeted stone-dissolving therapy.

5. CONCLUSIONS

1. Citric acid significantly enhances the solubility of both calcium salts through complex formation. The optimal dissolution range is pH 4–6 at a citrate concentration of 1.0–2.0 mM. Under identical conditions, calcium phosphate dissolves 1.4–1.6 times more actively than calcium oxalate, a difference attributed to the additional protonation of phosphate ions.
2. Dissolution is spontaneous and endothermic ($\Delta G^\circ < 0$, $\Delta H^\circ > 0$, $\Delta S^\circ > 0$) and is diffusion-controlled (Higuchi model, $R^2 > 0.98$). The dissolution rate of calcium phosphate is higher (k_H = 12.63 vs. 8.74 $mg \cdot L^{-1} \cdot h^{-1/2}$). Citrate adsorption on the crystal surface follows the Langmuir isotherm ($R^2 \approx 0.99$), with calcium phosphate exhibiting both higher capacity (Qmax) and greater affinity (K_L).
3. At physiological pH values of 5–6, 52–66% of calcium exists in the form of citrate complexes; this effectively reduces the activity of free Ca^{2+} ions and decreases urinary supersaturation. These findings establish a robust physicochemical basis for optimizing the prevention and treatment of urolithiasis using citrates, thereby validating current clinical practice. 6.

Declarations

Conflict of interest.

The authors declare no conflict of interest regarding this study.

Funding:

This study received no funding.

Author Contribution

F.B. and N.M. conceived and designed the study. F.B., A.M., S.I., and B.I. performed the experiments and collected the data. F.B., A.M., and B.I. conducted the thermodynamic, kinetic, and adsorption analyses. J.N. and S.I. contributed to the clinical interpretation and urolithiasis prophylaxis aspects. N.M. supervised the project. F.B. wrote the first draft of the manuscript. All authors discussed the results, critically revised the manuscript, and approved the final version. F.B. is the corresponding author and takes responsibility for the integrity of the work.CRediT authorship contribution statement:Conceptualization: F.B., N.M.Methodology: F.B., A.M., B.I.Validation: S.I., B.I.Formal analysis: F.B., A.M.Investigation: F.B., A.M., S.I., B.I.Resources: N.M., J.N.Data curation: F.B., A.M.Writing – original draft: F.B.Writing – review & editing: All authorsVisualization: F.B., A.M.Supervision: N.M., J.N.Project administration: F.B., N.M.Funding acquisition: NoneAll authors have read and approved the final manuscript.

Acknowledgement

The authors express their sincere gratitude to Samarkand State University named after Sharof Rashidov and Samarkand State Medical University for scientific and organizational support. The authors also thank the staff of the laboratories and departments where the experimental work was carried out for their technical assistance and helpful discussions.

References

1. Romero V, Akpinar H, Assimos DG (2010) Kidney stones: a global picture of prevalence, incidence, and associated risk factors. Rev Urol 12:e86. https://doi.org/10.3909/riu0459
2. Evan AP (2010) Physiopathology and etiology of stone formation in the kidney and the urinary tract. Pediatr Nephrol 25:831–841. https://doi.org/10.1007/s00467-009-1116-y
3. Scales CD Jr et al (2012) Prevalence of kidney stones in the United States. Eur Urol 62:160–165. https://doi.org/10.1016/j.eururo.2012.03.052
4. Daudon M, Bazin D, Letavernier E (2015) Randall's plaque as the origin of calcium oxalate kidney stones. Urolithiasis 43(Suppl 1):5–11. https://doi.org/10.1007/s00240-014-0703-y
5. Pak CY (1987) Citrate and renal calculi. Min Electrolyte Metab 13:257–266. https://doi.org/10.1016/S0272-6386(12)80635-4
6. Tiselius HG (2003) Epidemiology and medical management of stone disease. BJU Int 91:758–767. https://doi.org/10.1046/j.1464-410X.2003.04208.x
7. Nurillaev ZhYa N, KhZh, Berdimurodova FP, Mukhamadiev NK (2023) Evaluation of therapeutic and metaphylactic measures in urolithiasis depending on the stone composition. Med Bull

Bashkortostan 18:24–28. https://mvb-bsmu.ru/files/journals/1_2023.pdf

8. Coe FL, Worcester EM, Evan AP (2016) Idiopathic hypercalciuria and formation of calcium renal stones. Nat Rev Nephrol 12:519–533. https://doi.org/10.1038/nrneph.2016.101
9. Hesse A, Heimbach D (1999) Causes of phosphate stone formation and the importance of metaphylaxis by urinary acidification: a review. World J Urol 17:308–315. https://doi.org/10.1007/s003450050152
10. Barcelo P et al (1993) Randomized double-blind study of potassium citrate in idiopathic hypocitraturic calcium nephrolithiasis. J Urol 150:1761–1764. https://doi.org/10.1016/S0022-5347(17)35888-3
11. Ettinger B et al (1997) Potassium-magnesium citrate is an effective prophylaxis against recurrent calcium oxalate nephrolithiasis. J Urol 158:2069–2073. https://doi.org/10.1016/S0022-5347(01)68155-2
12. Pak CYC et al (1985) Long-term treatment of calcium nephrolithiasis with potassium citrate. J Urol 134:11–19. https://doi.org/10.1016/S0022-5347(17)46962-X
13. Ryall RL (1997) Urinary inhibitors of calcium oxalate crystallization and their potential role in stone formation. World J Urol 15:155–164. https://doi.org/10.1007/BF02201852
14. Kok DJ, Papapoulos SE, Bijvoet OLM (1990) Crystal agglomeration is a major element in calcium oxalate urinary stone formation. Kidney Int 37:51–56. https://doi.org/10.1038/ki.1990.7
15. Hess B et al (2000) Citrate determines calcium oxalate crystallization kinetics and crystal morphology—studies in the presence of Tamm–Horsfall protein of a healthy subject and a severely recurrent calcium stone former. Nephrol Dial Transpl 15:366–374. https://doi.org/10.1093/ndt/15.3.366
16. Daudon M, Jungers P (2004) Clinical value of crystalluria and quantitative morphoconstitutional analysis of urinary calculi. Nephron Physiol 98:p31–p36. https://doi.org/10.1159/000080261
17. Bakker E, Pretsch E (2005) Potentiometric sensors for trace-level analysis. TrAC Trends Anal Chem 24:199–207. https://doi.org/10.1016/j.trac.2005.01.003
18. Smith RM, Martell AE, Motekaitis RJ (2004) NIST standard reference database 46. *NIST critically selected stability constants of metal complexes database Ver*, *2*. nist.gov/system/files/documents/srd/46_8.htm
19. Gregory TM, Moreno EC, Brown WE (1970) Solubility of $CaHPO_4{\cdot}2H_2O$ in the system $Ca(OH)_2$–H_3PO_4–H_2O at 5, 15, 25, and 37.5°C. J Res Natl Bur Stand Phys Chem 74:461. https://doi.org/10.6028/jres.074A.036
20. Tomazic B, Nancollas GH (1979) The kinetics of dissolution of calcium oxalate hydrates. J Cryst Growth 46:355–361. https://doi.org/10.1016/0022-0248(79)90083-6
21. Sheehan ME, Nancollas GH (1984) The kinetics of crystallization of calcium oxalate trihydrate. J Urol 132:158–163. https://doi.org/10.1016/S0022-5347(17)49510-3

22. Chien SH (1993) Solubility assessment for fertilizer containing phosphate rock. Fertil Res 35:93–99. https://doi.org/10.1007/BF00750223
23. Van Cappellen P et al (1993) A surface complexation model of the carbonate mineral-aqueous solution interface. Geochim Cosmochim Acta 57:3505–3518. https://doi.org/10.1016/0016-7037(93)90135-J
24. Izatulina AR et al (2018) Hydrated calcium oxalates: crystal structures, thermal stability, and phase evolution. Cryst Growth Des 18:5465–5478. https://doi.org/10.1021/acs.cgd.8b00826
25. Haynes WM (ed) (2016) CRC handbook of chemistry and physics. CRC
26. Elliott JC (2013) Structure and chemistry of the apatites and other calcium orthophosphates, vol 18. Elsevier
27. Wyrzykowski D et al (2010) Thermodynamic interactions of the alkaline earth metal ions with citric acid. J Therm Anal Calorim 102:149–154. https://doi.org/10.1007/s10973-010-0970-y
28. Stumm W, Morgan JJ (2013) Aquatic chemistry: chemical equilibria and rates in natural waters. John Wiley Sons. https://doi.org/10.1007/s10973-010-0970-y
29. Burgot JL (2012) Ionic equilibria in analytical chemistry. Springer Science & Business Media
30. Sharp K (2001) Entropy—enthalpy compensation: Fact or artifact? Protein Sci 10:661–667. https://doi.org/10.1110/ps.37801
31. Wang L, Nancollas GH (2008) Calcium orthophosphates: crystallization and dissolution. Chem Rev 108:4628. https://doi.org/10.1021/cr0782574
32. Pak CYC (1998) Kidney stones. Lancet 351:1797–1801. https://doi.org/10.1016/S0140-6736(98)01295-1
33. Curhan GC et al (1993) A prospective study of dietary calcium and other nutrients and the risk of symptomatic kidney stones. N Engl J Med 328:833–838. https://www.nejm.org/doi/abs/10.1056/NEJM199303253281203
34. Dokoumetzidis A, Macheras P (2006) A century of dissolution research: from Noyes and Whitney to the biopharmaceutics classification system. Int J Pharm 321:1–11. https://doi.org/10.1016/j.ijpharm.2006.07.011
35. Uskokovic V (2015) Nanostructured platforms for the sustained and local delivery of antibiotics in the treatment of osteomyelitis. Crit Rev Ther Drug Carrier Syst 32. https://doi.org/10.1615/CritRevTherDrugCarrierSyst.2014010920
36. De Yoreo JJ, Qiu SR, Hoyer JR (2006) Molecular modulation of calcium oxalate crystallization. Am J Physiol Ren Physiol 291:F1123–F1132. https://doi.org/10.1152/ajprenal.00136.2006
37. Jung T, Sheng X, Choi CK, Kim WS, Wesson JA, Ward MD (2004) Probing crystallization of calcium oxalate monohydrate and the role of macromolecule additives with in situ atomic force microscopy. Langmuir 20:8587–8596. https://doi.org/10.1021/la0488755
38. UK NGC et al (2019) Prevention of recurrence. NICE Guideline Template

39. Pak CYC, Sakhaee K, Fuller C (1986) Successful management of uric acid nephrolithiasis with potassium citrate. Kidney Int 30:422–428. https://doi.org/10.1038/ki.1986.201
40. Allie S, Rodgers A (2003) Effects of calcium carbonate, magnesium oxide and sodium citrate bicarbonate health supplements on the urinary risk factors for kidney stone formation. Clin Chem Lab Med 41(1):39–45
41. Scoglio M, Bargagli M, Fuster DG (2026) Magnesium and kidney stones: a concise narrative review. Clin Kidney J sfag 248. https://doi.org/10.1093/ckj/sfag248
42. Grases F, Costa-Bauza A, Prieto RM (2006) Renal lithiasis and nutrition. Nutr J 5:23. https://doi.org/10.1186/1475-2891-5-23
43. Khan SR et al (2016) Kidney stones. Nat Rev Dis Primers 2:16008. https://doi.org/10.1038/nrdp.2016.8
44. Pak CY (1994) Citrate and renal calculi: an update. Miner Electrolyte Metab 20:371–377

Figures

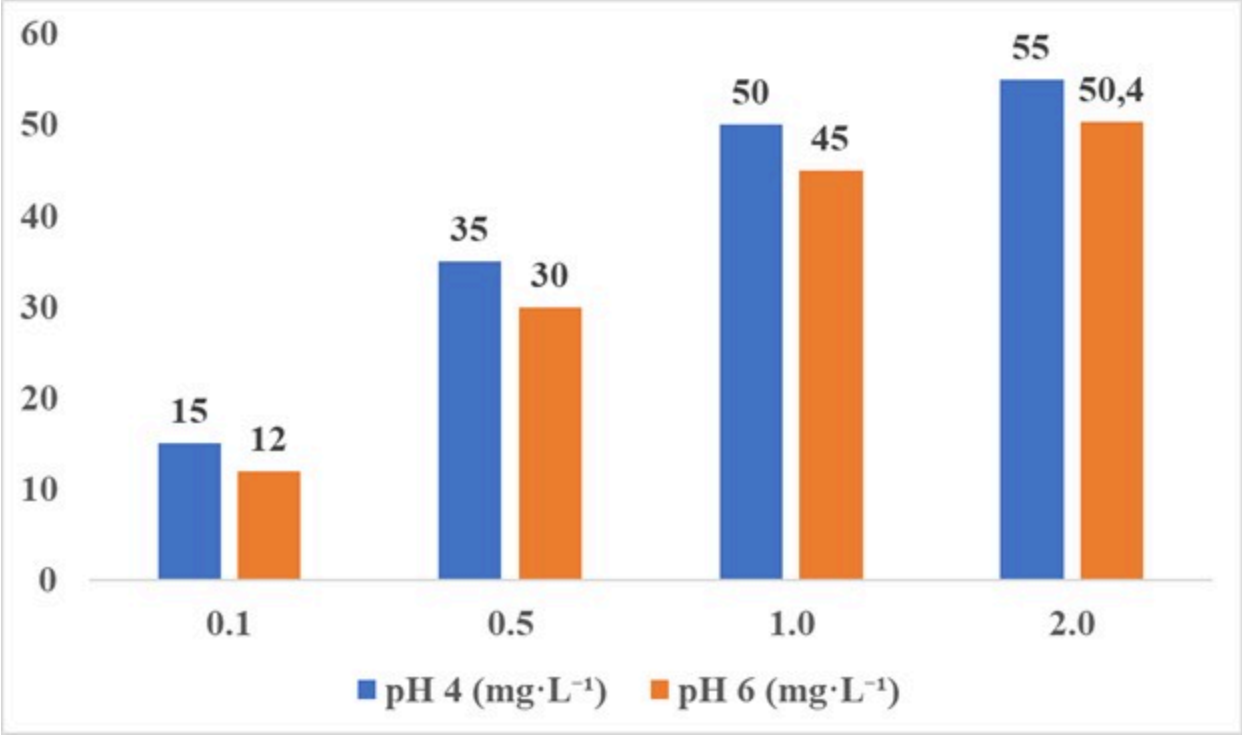


Figure 1

Histogram showing the solubility of calcium oxalate at pH 4 and pH 6 as a function of citrate content.

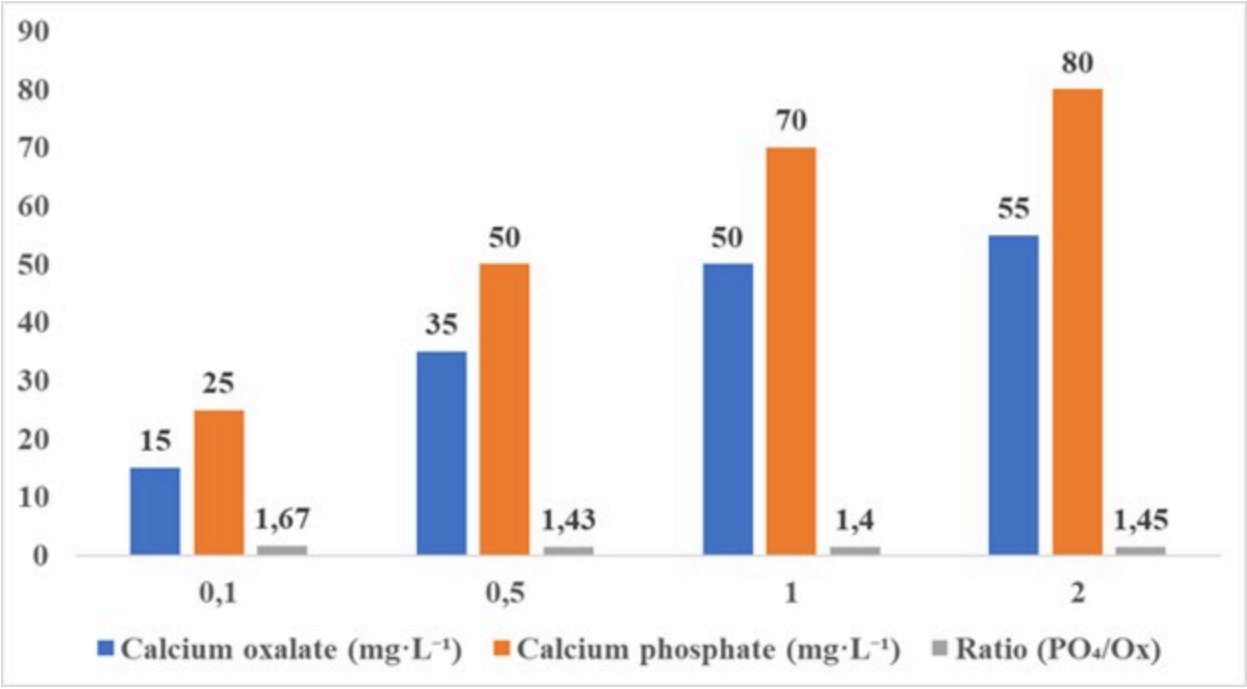


Figure 2

Comparison chart of two salts at pH 4 (bar chart).